

Article

Mechanical Properties Analysis of an Al-Mg Alloy Connecting Rod with Submicrometric Structure

Javier León †, Daniel Salcedo †*, Óscar Murillo †, Carmelo J. Luis †, Juan P. Fuertes †, Ignacio Puertas † and Rodrigo Luri †

Mechanical, Energetics and Materials Engineering Department, Public University of Navarre, Campus de Arrosadia, s/n, 31006 Pamplona, Spain; E-Mails: javier.leon@unavarra.es (J.L.); murillocrespo@gmail.com (O.M.); cluis.perez@unavarra.es (C.J.L.); juanpablo.fuertes@unavarra.es (J.P.F.); inaki.puerta@unavarra.es (I.P.); rodrigo.luri@unavarra.es (R.L.)

† These authors contributed equally to this work.

* Author to whom correspondence should be addressed; E-Mail: daniel.salcedo@unavarra.es; Tel.: +34-948-169-608; Fax: +34-948-169-099.

Academic Editor: Hugo F. Lopez

Received: 22 June 2015 / Accepted: 27 July 2015 / Published: 31 July 2015

Abstract: Over these last few years, there has been a growing interest in developing mechanical components from submicrometric materials due to the significant improvement that these materials present compared to their original state. This present research work deals with the study of the mechanical properties of a connecting rod isothermally forged from different starting materials. These materials are as follows: annealed aluminum alloy (AA) 5754, the same alloy previously deformed through equal channel angular pressing (ECAP) and a third case where the previously ECAP-processed material is subjected to a recovery heat treatment. A comparison is made between finite volume (FV) simulations and experimental tests with respect to hardness, plastic strain and forging force. Furthermore, the improvement in the mechanical properties of the connecting rod forged from predeformed material is evaluated in comparison to the connecting rod forged with annealed material. The microstructure of both cases is also compared at the end of the manufacturing process.

Keywords: ECAP; isothermal forging; microhardness; FV; heat treatment

1. Introduction

Over these last few years, there has been a large amount of research work on the application of severe plastic deformation (SPD) processes in order to improve the mechanical properties of materials and to reduce their grain size [1]. Nevertheless, in spite of the large number of studies that analyze the improvement in mechanical properties and microstructure, there are only a few studies that are focused on the application of these materials to the manufacturing of mechanical components with submicrometric structure. The processes that are included in the SPD processes are those thermo-mechanical ones that are able to introduce high plastic strain values ($\epsilon \gg 1$) in the material. Due to this plastic strain introduced in the presence of a high hydrostatic pressure, materials with a submicrometric structure may be obtained in the case of metallic alloys [2]. Among the improvements in the mechanical properties, the following stand out: an increase in the yield and in the tensile strength, improvement in fatigue resistance and in forgeability and, under specific conditions, superplastic behavior [3,4]. Other material properties affected by the use of SPD processes are corrosion [5].

Among SPD processes, the so-called equal channel angular pressing (ECAP) is of special interest [6]. ECAP is a discontinuous process that consists of exerting a compression force on a material to make it flow through a die. This ECAP die consists of two channels with approximately the same cross-section that intersect at an angle between 90° and 120° . ECAP has noticeably evolved over these last few years with the aim of obtaining a uniform material flow and, at the same time, optimizing the imparted strain and avoiding any damage to the material. To this end, it is necessary to consider tangent fillet radii between both channels of the ECAP die [7]. Moreover, as mentioned earlier, thanks to this process, a noticeable reduction in the grain size may be obtained for the metallic alloys processed [8].

The grain size reduction and the previous deformation value may make phenomena, such as dynamic recrystallization and recovery, appear. These are natural softening processes that take place during the hot deformation of materials, and they are essential, because they reduce both the material stresses and the force required to deform the material. In addition, they have a great deal of influence on the final microstructure and mechanical properties. Therefore, microstructure evolves when plastic strain is introduced, thus forming subgrains in bands aligned with planes with the highest shear stress and increasing the dislocation density until a balance is reached where the dislocation density remains constant and there is no evolution in the subgrains [9].

On the other hand, a drawback of this kind of process is the amount of material required for some products. Therefore, a scaling up of this process is essential for its use in industry [10].

It is well known that the influence of crystalline structure, previous heat treatments and the processes undergone by the material to be forged on forgeability is essential to achieve success in the forging process [11]. For that reason, the application of these kinds of materials to the forging process may be interesting.

Most of the studies on previously ECAP-processed materials deal with the compression of different alloys between plane-shape dies [12,13]. In some of them, temperature is taken into account as a study variable, which involves a higher degree of difficulty as the recrystallization process is eased [14].

Among the research work in which the ECAP process and forging are combined, that from Lee *et al.* [15] is noteworthy. These researchers study the manufacturing of an impeller from a previously ECAP-processed aluminum-zinc (AZ) 31 magnesium alloy, which leads to an optimum die filling,

a lesser flash amount and a result closer to the required final shape. Among the most relevant mechanical components that have been developed, the application of ECAP and a subsequent forging process in order to manufacture bolts is also interesting [16,17]. These authors analyze and compare the microhardness of the manufactured bolts, and tension tests are performed, thus concluding that the ECAP-processed materials have a better forgeability and hardness. In addition, other components, such as rings [18], blades [19] and gears [20], have also been manufactured from these materials, where this always leads to an improvement, both in hardness and in mechanical strength for the mechanical components forged from previously ECAP-processed material.

Connecting rods are very widespread industrial mechanical components that allow us to transform an axial rotatory movement into an alternative linear movement. In most cases, forging or casting is used in its manufacturing, followed by a machining process for the zones where higher precision is needed. Diverse designs of dies and rolls have been studied by finite element simulations [21,22]. The velocity to which these components are subjected makes a big reduction in the mechanism inertial forces possible, if a lower weight is achieved in the component. There are a large number of technical papers that deal with the optimization of the connecting rod geometry by reducing its central section and the section at the heads [23,24]. In this case, it is very important to evaluate the fatigue behavior and the possible buckling. Moreover, studies on different methods to decrease the friction coefficient between the connecting rod heads and the shaft are found in the bibliography [25], as well as redesigns in order to improve the fatigue behavior by reducing the contact pressure of the heads with the shaft [26].

Nevertheless, no studies have been found on the use of previously ECAP-processed materials for the manufacturing of connecting rods, which would greatly decrease the weight of these components. For this reason, connecting rods constitute a potential mechanical component whose mechanical properties would be improved if the double deformation process proposed in this present research work is applied to them.

2. Experimental Section

This present section outlines the manufacturing process of the connecting rods, the study designed in order to obtain them at different temperature values, the study of the mechanical properties for the connecting rod forged at the optimum temperature in detail and the finite volume simulations with which experimental results are to be compared.

2.1. Manufacturing of the Connecting Rods

First of all, the procedure carried out in order to obtain the connecting rods that are to be subsequently tested is shown. The starting material is a 5754 aluminum alloy, which is manufactured in the form of an extruded rod with a diameter of 20 mm, as is shown in Figure 1a. Once manufactured, a heat treatment of annealing is performed: furnace temperature is increased from room temperature to 345 °C during 1 h, then it is maintained during 2 h, and finally, the material is slowly cooled down to room temperature with a cooling slope of no more than 20 °C per hour.

Subsequent to the annealing heat treatment, the material is ECAP processed in a press designed for this purpose. Route C is selected as the ECAP processing route, and two passages (N2) are performed, which means that the billet is rotated 180° along the extrusion direction between each passage.

Afterwards, as is observed in Figure 1b, the ECAP-processed billets are turned by removing the billet zones that have not undergone severe plastic deformation. At the next stage, the billets are machined with a computerized numerical control (CNC) lathe into the shape shown in Figure 1c, which is designated as the preform and from which the forging process is carried out [27]. The forging of the connecting rod is performed in two strokes. Before carrying out the first stroke, the preform is introduced in the forging dies heated at the required temperature. It takes five minutes to reach the specified temperature for the whole billet, and then, the forging process takes place. The outer shape is achieved with the first stroke (Figure 1d), whereas the inner cavities are performed with the second stroke, as is shown in Figure 1e. Finally, flash is removed with the use of a milling machine, and the two holes where the shafts will be housed are drilled [28].

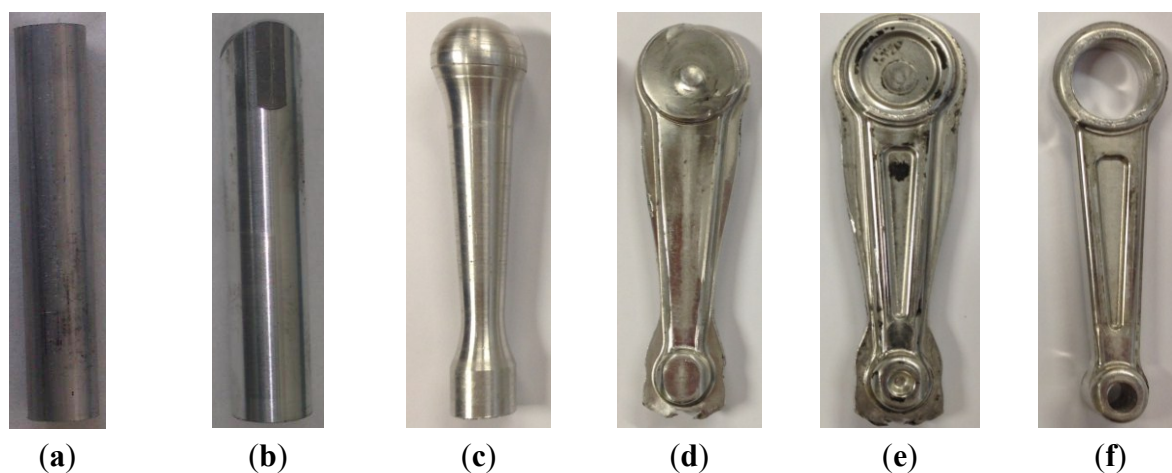


Figure 1. Stages followed in the manufacturing of the connecting rods: (a) N0; (b) N2; (c) Preform; (d) first stroke; (e) second stroke; (f) final shape.

2.2. Design of the Forging Study at Different Temperature Values

Due to the difference in plastic strain that exists at the different zones of the connecting rod, three study zones are selected in order to perform the Vickers microhardness measurements (Hv). The three selected zones are as follows: the two heads and the body zone with the highest plastic strain value, as shown in Figure 2.

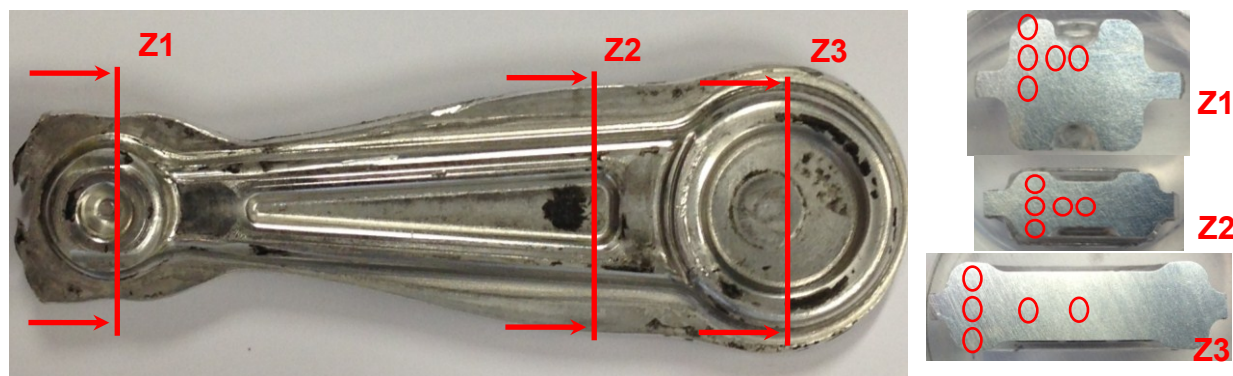


Figure 2. Selected study zones to be cut and points where Vickers microhardness (Hv) is measured.

The forging of the connecting rods is carried out both for the material with no previous accumulated plastic strain (N0) and for the material previously ECAP processed (N2) at room temperature. The temperatures initially selected for both starting states are as follows: 100 °C, 150 °C, 200 °C and 250 °C.

In each of the three selected study zones, five points are again selected where microhardness measurements are taken. In order to get these measurements, each of the study zones from Figure 2 are cut, embedded into a resin and polished until a mirror-like surface is achieved. Table 1 shows the results of the microhardness measurements for each of the connecting rods forged in the N0 state at the previously-mentioned temperature values.

Table 1. Microhardness values for the N0 forged connecting rods.

Temperature	100 °C			150 °C			200 °C			250 °C			
	Zone	Z1	Z2	Z3	Z1	Z2	Z3	Z1	Z2	Z3	Z1	Z2	Z3
Hv1		69.5	82.5	91.1	68.8	92.9	85.7	62.7	78.7	82.0	50.6	77.9	71.6
Hv2		73.3	85.3	86.6	69.1	86.9	87.5	51.6	79.6	83.2	-	70.8	72.9
Hv3		72.7	86.1	88.4	80.2	88.3	84.7	73.4	80.1	82.3	64.7	75.6	68.4
Hv4		72.2	96	96.5	74.7	98.9	89.0	72.9	86.9	79.2	59.1	77.4	71.3
Hv5		68.6	98.9	93.5	72.5	99.7	87.5	57.8	89.6	84.1	-	81.1	72.5
Mean		71.3	89.8	91.2	69.2	93.3	86.9	63.7	83.0	82.2	58.1	76.6	71.3
Standard Deviation		2.1	7.2	3.9	11.6	5.9	1.7	9.5	4.9	1.8	7.1	3.8	1.8

At a temperature of 250 °C in Zone 1, given the high material ductility, some of the measurements cannot be carried out, because the pyramidal shape of the indentation does not have the appropriate shape. Taking Table 1 into account, the optimum forging temperature selected for the N0 connecting rod turns out to be 100 °C, as it is the one with the highest microhardness values and with no cracks. Moreover, Table 2 shows the microhardness measurements for each of the N2 forged connecting rod (previously ECAP processed) at the previously-mentioned temperature values.

Table 2. Microhardness values for the N2 forged connecting rods.

Temperature	100 °C			150 °C			200 °C			250 °C			
	Zone	Z1	Z2	Z3	Z1	Z2	Z3	Z1	Z2	Z3	Z1	Z2	Z3
Hv1		109.2	110.4	104.5	101.8	106.2	97.7	96.3	91.9	99.7	83.4	82.9	80.5
Hv2		111.7	123.9	108.6	102.5	106.6	102.2	96.4	94.6	94.9	84.6	81.0	82.4
Hv3		106.9	119.5	109.4	103.4	110.7	105.2	97.9	85.0	95.6	86.9	85.0	80.8
Hv4		109.5	134.1	117.4	103.2	109.9	106.1	99.8	104.0	100.2	83.0	84.3	85.3
Hv5		110.8	124.1	113.8	100.7	132.0	106.6	99.5	109.8	101.4	79.6	85.8	82.0
Mean		109.6	125.7	110.7	102.3	113.1	103.6	98.0	97.1	98.4	83.5	83.8	82.2
Standard Deviation		1.8	11.2	5.0	1.1	10.8	3.7	1.7	9.9	2.9	2.7	1.9	1.9

Figure 3 shows a plot from the values shown in Tables 2 and 3. It may be seen that there is a drop in microhardness for N2 between 150 °C and 200 °C, thus obtaining values that are similar to N0. In addition, there are no cracks in the case of the connecting rod forged from pre-deformed material (N2), only for the temperature value of 250 °C.

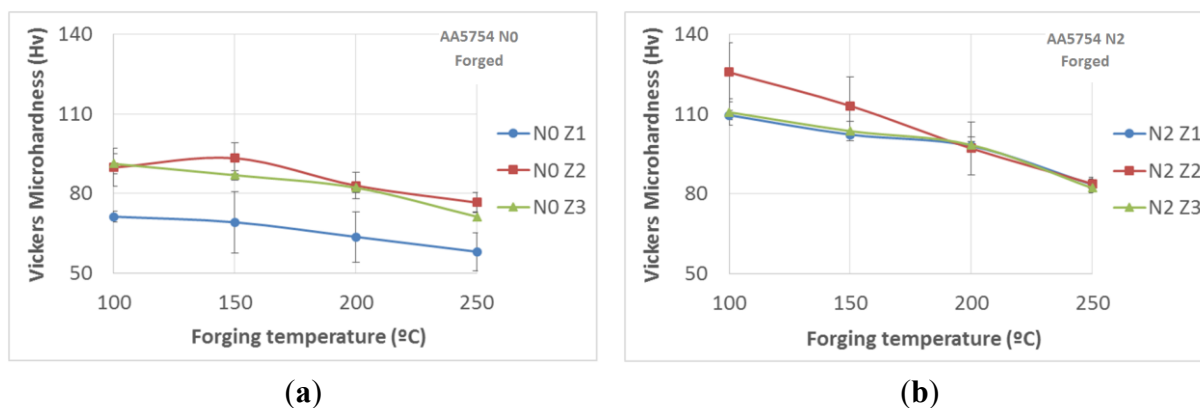


Figure 3. Hv microhardness vs. forging temperature for N0 and N2 states: (a) N0; (b) N2.

Taking these previous results into consideration, it is best to do a heat treatment for the preform (Figure 1c) before the isothermal forging process. This short recovery heat treatment consists of a temperature increase from room temperature to a high temperature with a heating rate of 12 °C/min, no maintenance time and a fast water cooling. To this end, the following treatment temperature values are selected: 240 °C, 260 °C, 280 °C, 300 °C and 320 °C. From here on, this heat treatment will be known as the flash treatment. The aim is to achieve stress relief, but with no recrystallization for the material microstructure, since most of the improvement in the mechanical properties introduced by ECAP would be lost. In order to study the microhardness after each recovery treatment, samples from the ECAP-processed material are taken. Five microhardness measurements (Hv) are carried out on each sample with a different flash treatment, thus obtaining the mean and the standard deviation values for each study temperature, as shown in Table 3.

Table 3. Hv microhardness for the N2 state material after the flash treatment.

Temperature	240 °C	260 °C	280 °C	300 °C	320 °C
Hv1	100.6	98.4	96.7	89.6	63.8
Hv2	100.1	98.5	99.5	89.7	64.8
Hv3	97.6	98.2	97.5	92.5	63.6
Hv4	98.6	98.1	96.6	91.7	66.6
Hv5	97.2	97.9	97.2	89.8	64.0
Mean	98.8	98.2	97.5	90.7	64.6
Standard Deviation	1.5	0.2	1.2	1.3	1.2

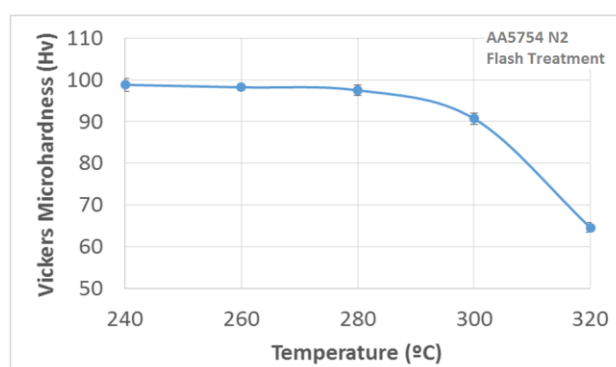


Figure 4. Hv microhardness vs. flash treatment temperature for the N2 starting state.

If the values from Table 3 are plotted, Figure 4 is attained, where it may be observed that there is a drop in the microhardness values, which starts from 280 °C, where this drop becomes significant at a temperature of 320 °C.

As is well known, SPD processes lead to a grain size refinement as a consequence of the severe plastic deformation that is imparted to the processed materials [4]. In this present study, the SPD process known as ECAP is used after two passages, and as can be observed in Figure 5b, there are a large number of deformation bands inside the former grains. These grains present a similar pattern to that shown in Figure 5a, because of Route C. However, deformation values are close to $\epsilon = 2.3$ [7]. This material is not suitable for forging purposes in this present state as a consequence of the formation of cracks when the connecting rod is to be forged. Therefore, a partial recovery heat treatment is employed in order to obtain a submicrometric structure that is partially recrystallized, which can be forged into the desired part.

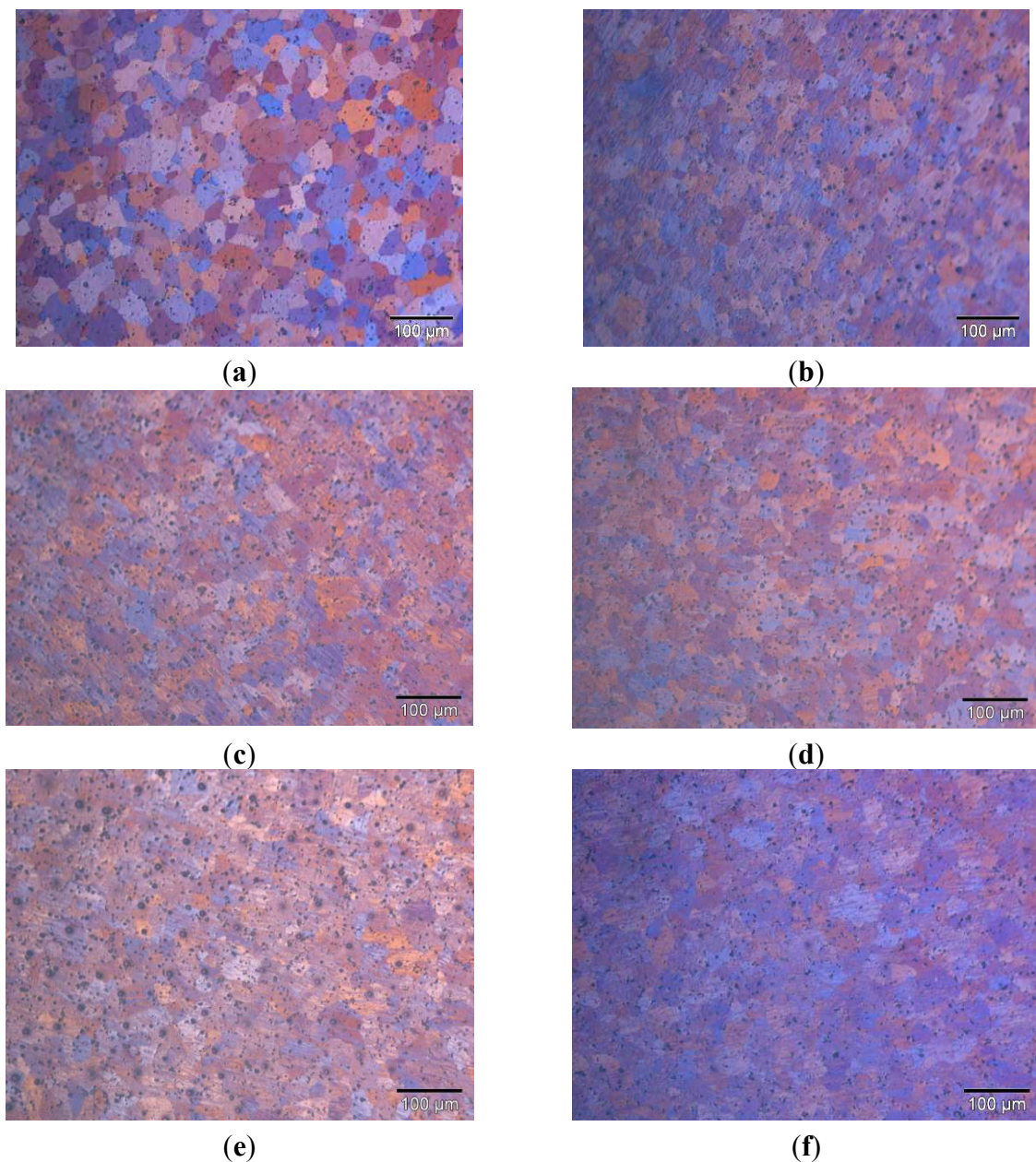
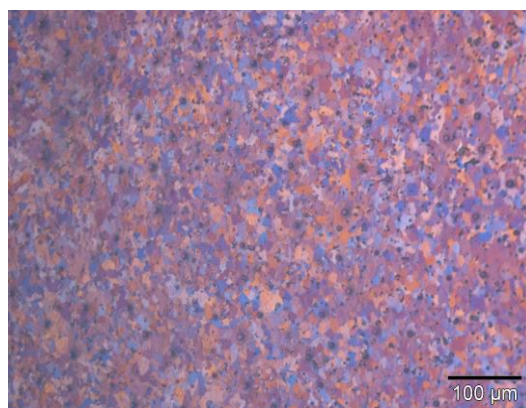


Figure 5. Cont.



(g)

Figure 5. Optical micrographs for the N2 state material after the flash treatment (tr): (a) N0; (b) N2; (c) N2 + flash tr. = 240 °C; (d) N2 + flash tr. = 260 °C; (e) N2 + flash tr. = 280 °C; (f) N2 + flash tr. = 300 °C; (g) N2 + flash tr. = 320 °C.

Taking these previous results into account, flash heat treatments at 280 °C and at 300 °C are selected, and subsequently, three isothermal forging processes are carried out under the following conditions. After the flash treatment at 280 °C, the isothermal forging at 150 °C is performed (Case 1), and after the flash treatment at 300 °C, isothermal forging processes at temperatures of 100 °C and 150 °C are performed (Cases 2 and 3, respectively). The microhardness values measured from each of the three selected zones in the forged connecting rods are shown in Table 4.

Table 4. Microhardness values for the N2 state connecting rods forged after the flash treatment.

Temperature	Case 1			Case 2			Case 3		
	280 °C → 150 °C			300 °C → 100 °C			300 °C → 150 °C		
Zone	Z1	Z2	Z3	Z1	Z2	Z3	Z1	Z2	Z3
Hv1	96.3	103.0	96.6	90.1	100.8	94.4	93.0	100.6	97.6
Hv2	86.7	97.0	91.9	81.4	98.9	90.0	88.1	96.1	99.0
Hv3	95.4	98.5	97.1	90.8	96.4	95.6	94.6	93.9	101.4
Hv4	99.2	107.1	104.6	91.9	106.6	98.1	95.5	109.0	100.3
Hv5	101.3	112.9	104.6	92.7	101.0	98.7	96.7	113.5	104.2
Mean	95.8	103.7	99.0	89.4	100.7	95.4	93.6	102.6	100.5
Standard Deviation	5.6	6.5	5.5	4.6	3.8	3.5	3.3	8.4	2.5

Figure 6 shows the microhardness values for each of the above-mentioned three cases and for each of the three study zones.

The connecting rod isothermally forged after the flash treatment at 280 °C shows cracks, and as a consequence, the temperature value selected for the flash treatment is 300 °C, thus leading to an optimum temperature value for the subsequent forging process of the N2 state connecting rod, which turns out to be 150 °C. To sum up, a mean value of Hv 84.1 is obtained in the case of the connecting rod forged at 100 °C from the N0 state material, 83.2 Hv in the case of the forging at 250 °C from the N2 state and Hv 98.9 in the case of the flash treatment at 300 °C and the subsequent forging at 150 °C from the N2 state.

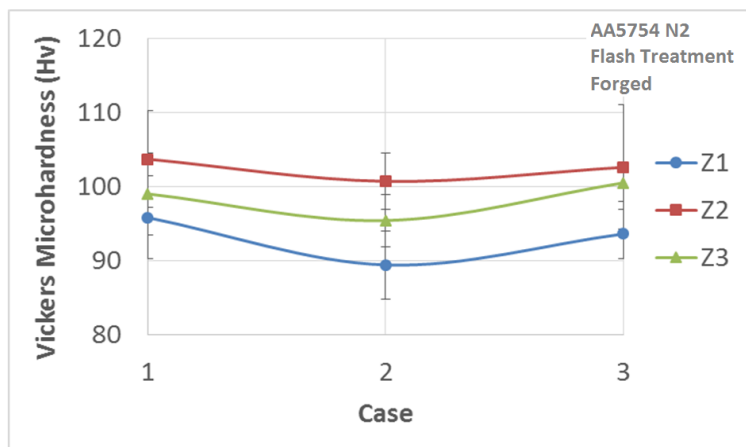


Figure 6. Microhardness values for the connecting rods forged after the three flash treatments selected.

Once the optimum forging temperature values are selected for each starting state (100 °C for the N0 state and 150 °C for the N2 state after the flash treatment at 300 °C), a detailed and profound study on microhardness is carried out for these two previously-mentioned cases. In order to do this, each connecting rod is longitudinally cut into four different zones, as can be observed in Figure 7a, and then embedded in resin and polished. The microhardness measurements are taken from the locations shown in Figure 7b.

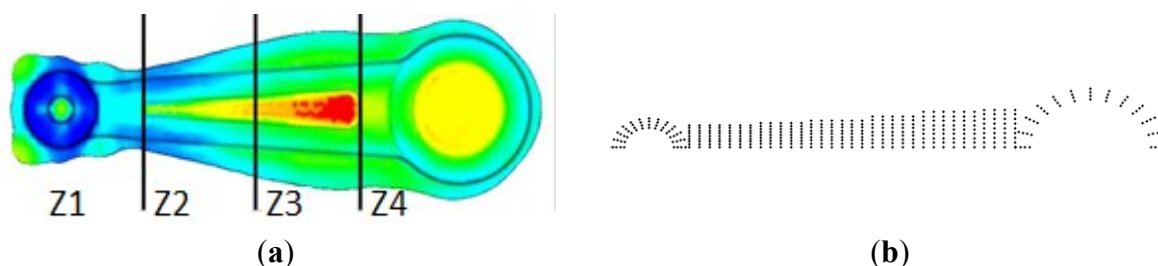


Figure 7. Selection of the locations where microhardness measurements are taken: (a) zones to be cut; (b) indentation points.

3. Results and Discussion

Microhardness values obtained in the previous section are plotted using MATLAB[®] (R2013b, MathWorks, Natick, United States, 1984) in order to be able to compare the pattern attained to the plastic strain calculated from the finite volume simulations [27,28]. Figure 8 shows the microhardness mapping obtained for the optimum connecting rod in each starting state.

It may be observed from Figure 8 that the connecting rod forged from previously ECAP-processed material presents higher microhardness values in all of the points under consideration, except at the left end of the small head. Taking into account the mean value of the microhardness measurements for each connecting rod, a value of Hv 89.1 is obtained for the connecting rod forged from the N0 state material and Hv 100.0 in the case of the N2 state with flash treatment.

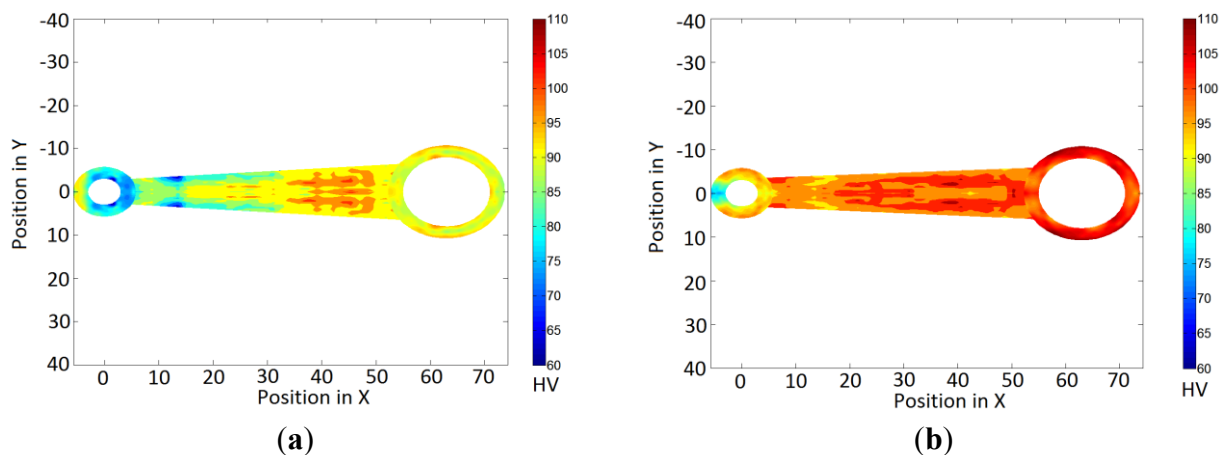


Figure 8. Microhardness values for the optimum connecting rod in each starting state: (a) N0 connecting rod forged at 100 °C; (b) N2 + flash tr. at 300 °C connecting rod forged at 150 °C.

Figure 9 shows the differences in microhardness for each optimum connecting rod. It should be underlined that the highest difference values are found at the small head zone (with the exception of its left end) and at the transition zone to the connecting rod central part. This previously-mentioned zone at the small head is the one that would undergo the highest stress values during the normal behavior of the mechanical component, and therefore, in the case of using the connecting rod forged from the predeformed material, its fatigue life would then be improved.

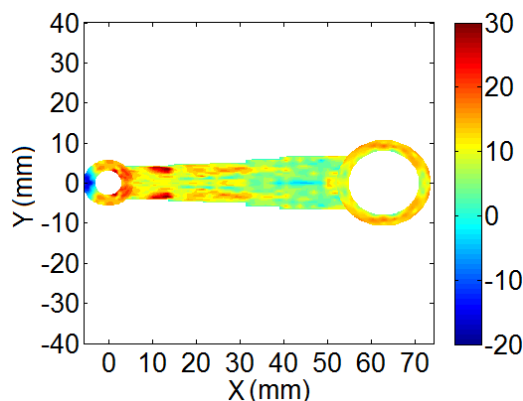


Figure 9. Differences in microhardness between the optimum connecting rods for each starting state.

It may be affirmed from Figure 8 that the microhardness distribution pattern is the same for both connecting rods: low values at the small head and high values at the big head. The zone with the highest values is found in the connecting rod body, but at an area close to the big head. Figure 10 shows the equivalent plastic strain attained at the longitudinal cross-section of the connecting rod and calculated by finite volume simulations [28] using simufact.forming[®] (12.0, MSC Software Corporation, Hamburg, Germany, 1999). It may be pointed out that the plastic strain distribution obtained in the FV simulations for both connecting rods is the same as that obtained from the microhardness measurements.

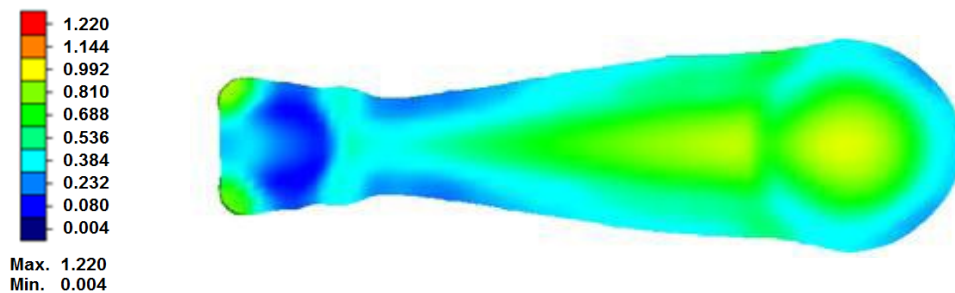


Figure 10. Connecting rod strain obtained by finite volume simulation [27].

Moreover, experimental forging forces are compared to those obtained from finite volume simulations. Hollomon-type flow rules are used in these FV simulations for each of the three material types employed: N0, N2 and N2 with flash treatment. To this end, different isothermal compression tests are performed [26]. As may be observed in Figure 11, the prediction of the maximum required force is precise both in the first and in the second stroke, although the shape for the load-stroke curve of the second stroke does not fit very well due to the different initial positioning in the FV simulations. In all cases, it is observed that the force required for the N2 material is the highest, whereas it turns out to be similar for N0 and N2 with flash treatment.

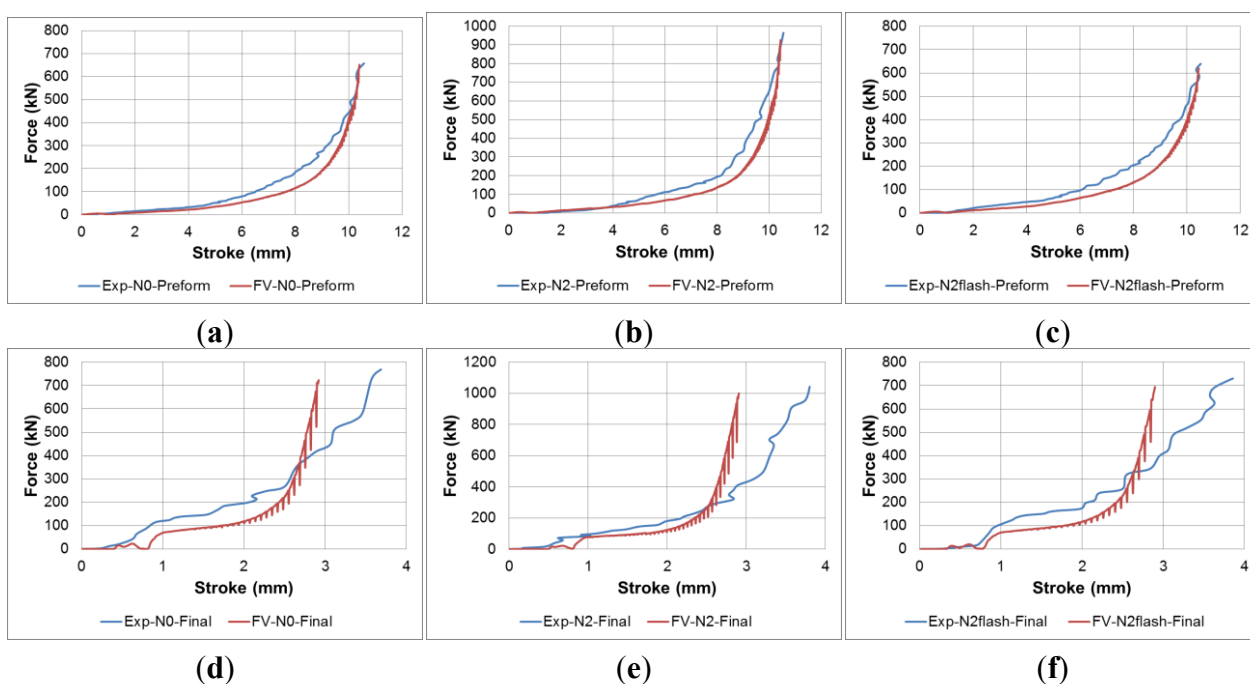


Figure 11. Comparison of the load-stroke curves: (a) N0 preform; (b) N2 preform; (c) N0 preform + flash tr.; (d) N0 final stroke; (e) N2 final stroke; (f) N2 + flash tr. final stroke.

Regarding optical microscopy, Figure 12 shows a series of optical micrographs for each zone from Figure 7, both for N0 and N2. It may be observed that Zones 1 and 2 show a lesser number of deformation bands in relation to Zones 3 and 4, both for connecting rods forged from N0 and N2. In all zones, there is a higher number of deformation bands in the case of the previously ECAP-processed material (N2).

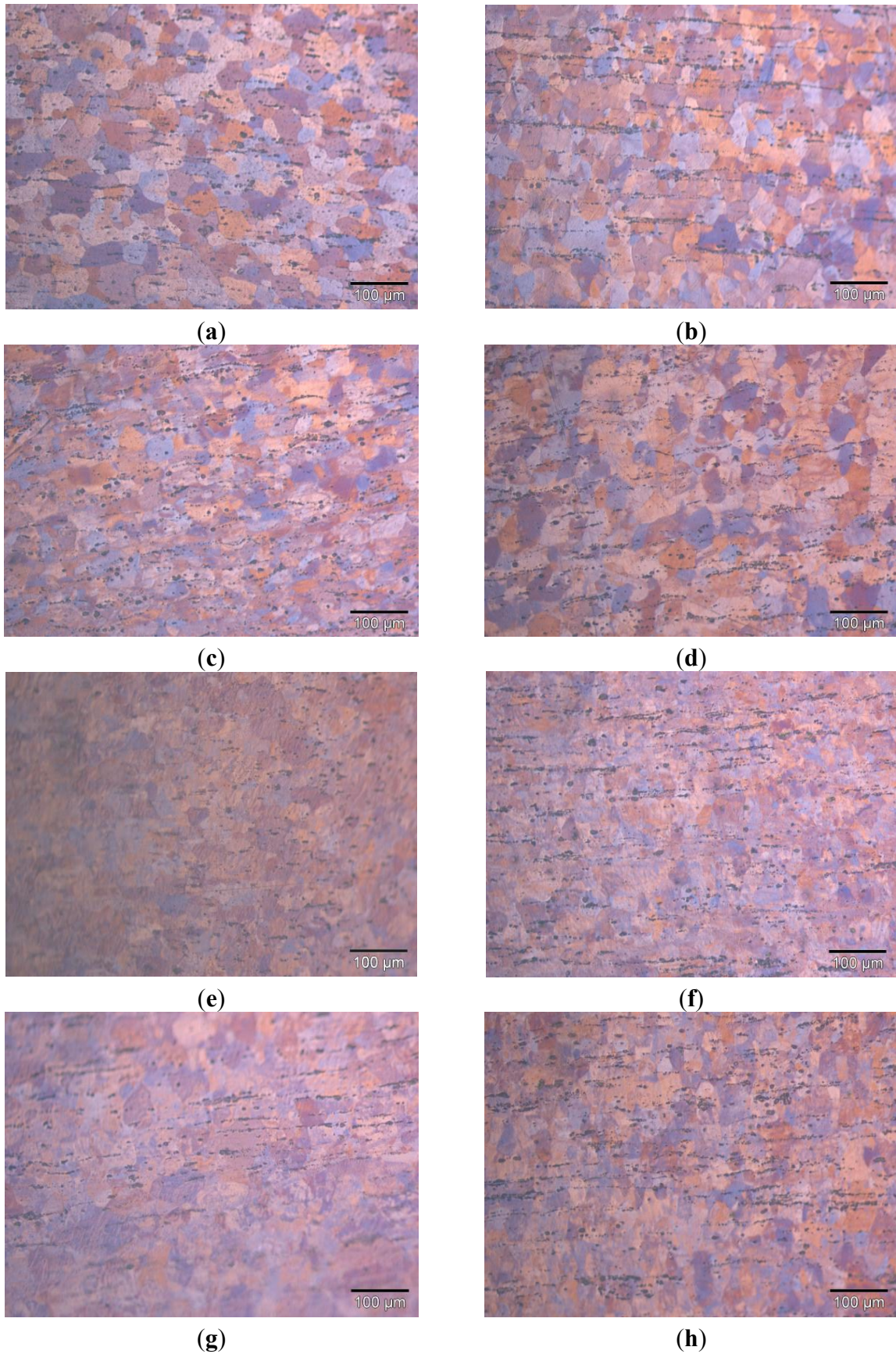
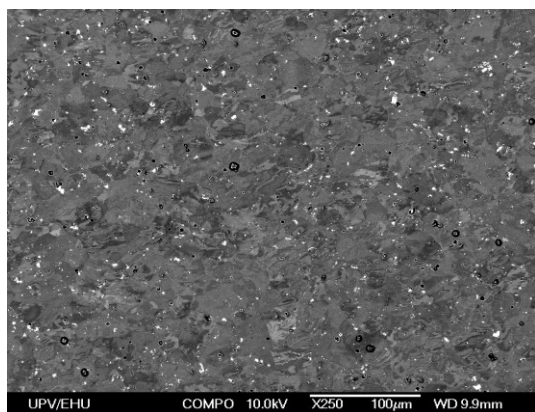
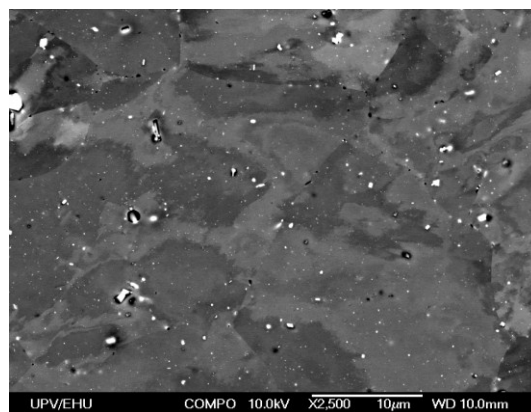


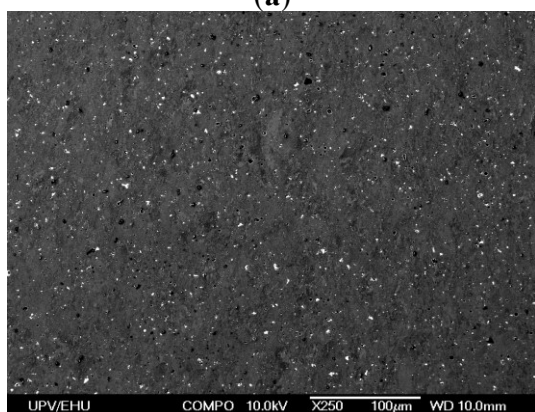
Figure 12. Optical micrographs of the connecting rods forged at the optimum temperature: (a) N0 – Z1; (b) N0 – Z2; (c) N0 – Z3; (d) N0 – Z4; (e) N2 – Z1; (f) N2 – Z2; (g) N2 – Z3; (h) N2 – Z4.



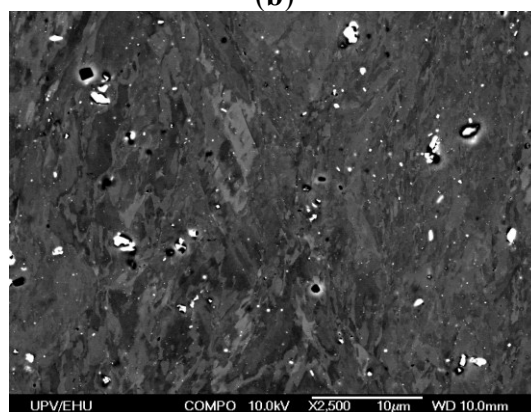
(a)



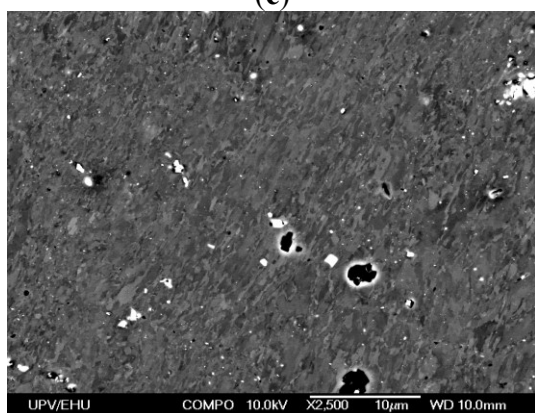
(b)



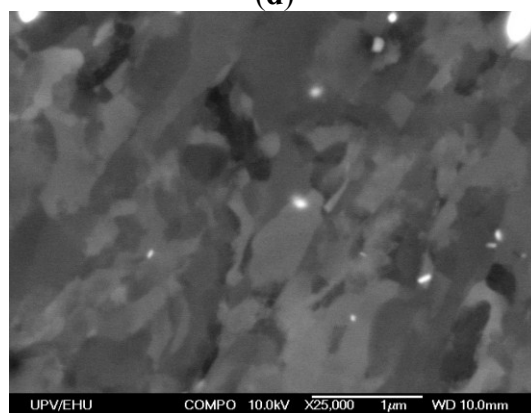
(c)



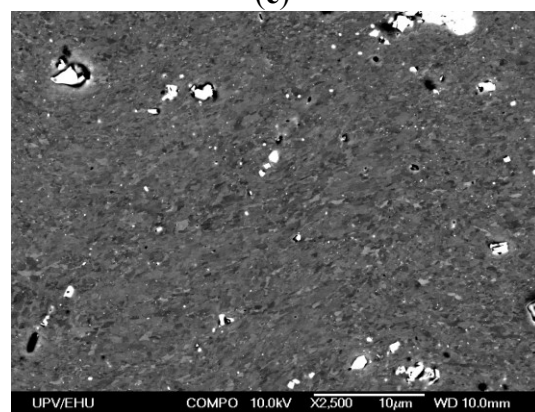
(d)



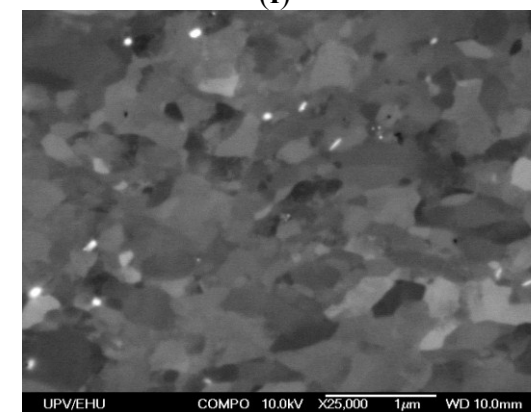
(e)



(f)



(g)



(h)

Figure 13. Cont.

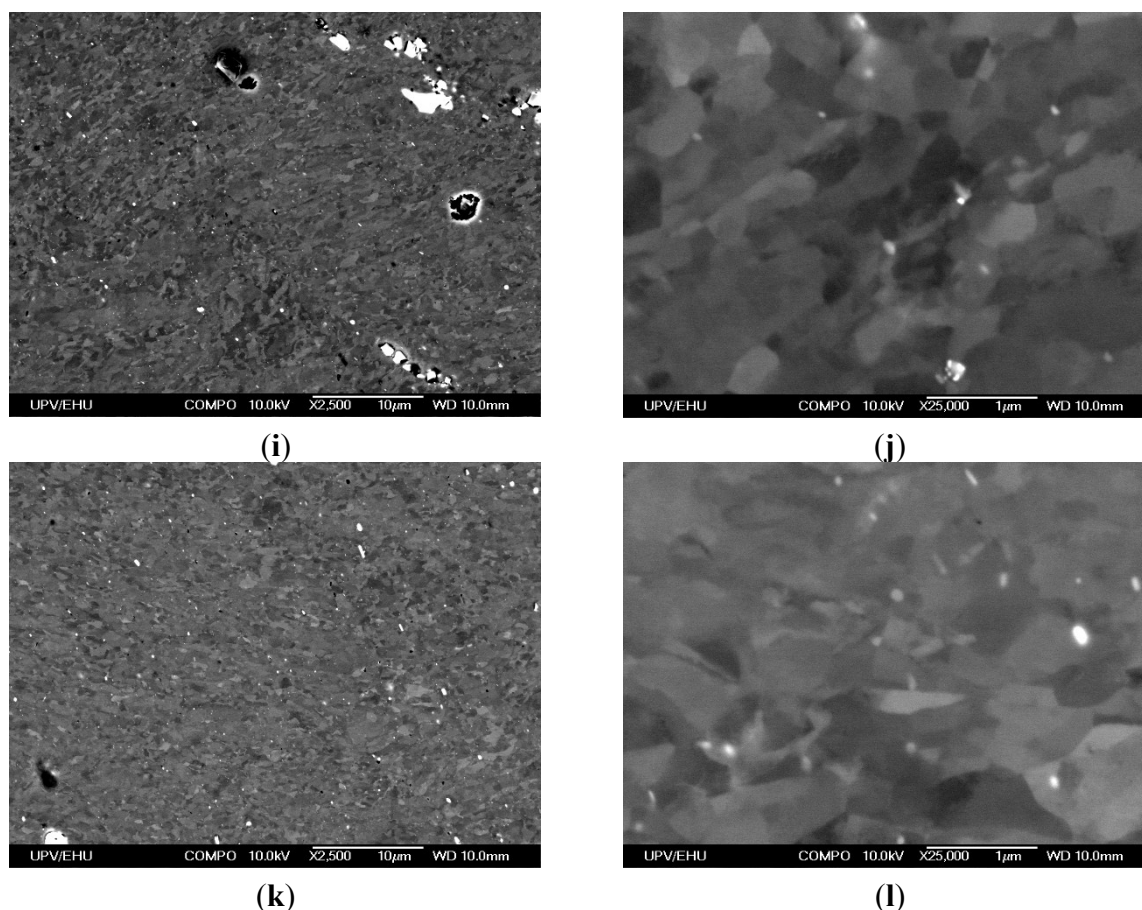


Figure 13. SEM micrographs of the connecting rods forged at the optimum temperature: (a) N0 – Z1; (b) N0 – Z1; (c) N0 – Z4; (d) N0 – Z4; (e) N2 – Z1; (f) N2 – Z1; (g) N2 – Z4; (h) N2 – Z4; (i) N2 + flash tr. – Z1; (j) N2 + flash tr. – Z1; (k) N2 + flash tr. – Z4; (l) N2 + flash tr. – Z4.

Finally, in order to assess the grain size and the material homogeneity, different SEM (SGIker, Leioa, Spain; technological center) micrographs are taken from Zones 1 and 4 in the connecting rods forged from the studied material states at their optimum forging temperature. It may be observed in the SEM micrographs at a lower magnification from Figure 13 that the microstructure homogeneity is better for the N2 and the N2 with flash treatment starting states. A smaller grain size is also observed, reaching a submicrometric level for the previously-mentioned cases, whereas grains with a much greater size are observed for N0. Furthermore, whereas a similar microstructure is observed at Zones 1 and 4 for the N2 and the N2 with flash treatment states, in the case of N0, the grains observed at Zone 1 are very heterogeneous and with a low deformation level, which will have an influence on the mechanical properties of the component to be forged.

4. Conclusions

In this present research work, a study on the forgeability of an AA5754 connecting rod is carried out starting from three different states: after an annealing heat treatment (N0), after having been previously deformed by ECAP twice (N2) with Route C and after the same previous case, but with an extra flash heat treatment at 300 °C prior to forging. Optimum forging temperature values have been determined

for connecting rods from the N0 state, N2 state and N2 state with flash treatment, which turn out to be 100 °C, 250 °C and 150 °C, respectively.

A microhardness value of Hv 89.1 is obtained for the connecting rod forged from the N0 state material. In the case of the N2 state with flash treatment, the value is 100.0 Hv, but there is an important improvement at the small head zone (except at its left end), which will lead to an improvement in its fatigue life.

It has been observed that the homogeneity in the microstructure is better for the N2 and N2 with flash treatment starting states. Furthermore, the grain size is smaller in these both cases, and it is reduced to a submicrometric level.

The variation pattern of microhardness throughout the connecting rod is very similar for N0 and N2 plus flash treatment cases, and this also agrees with the accumulated plastic strain calculated by finite volume simulations. Finally, the force obtained in the finite volume simulations has been compared with that from the experimental tests, achieving a good proximity to the maximum force required for the forging process.

Acknowledgments

The authors acknowledge the support given by the Ministerio de Ciencia e Innovación (Spain) (Research Project: DPI2013-41954-P).

Author Contributions

Although all of the authors of this present manuscript have contributed to most of the research tasks. In addition, the main tasks performed by each author are listed. Javier León, Daniel Salcedo and Carmelo J. Luis conceived and designed the experiments. Óscar Murillo and Juan P. Fuertes performed the experiments. Daniel Salcedo, Rodrigo Luri, Juan P. Fuertes and Óscar Murillo performed the FV simulations. Javier León and Óscar Murillo performed the MATLAB programming. Javier León, Daniel Salcedo and Carmelo J. Luis analyzed the data. Javier León, Daniel Salcedo, Carmelo J. Luis and Ignacio Puertas wrote the paper.

Conflicts of Interest

The authors declare no conflict of interest.

References

1. Valiev, R.Z.; Islamgaliev, R.K.; Alexandrov, I.V. Bulk nanostructured materials from severe plastic deformation. *Prog. Mater. Sci.* **2000**, *45*, 103–189.
2. Valiev, R.Z.; Langdon, T.G. Principles of equal-channel angular pressing as a processing tool for grain refinement. *Prog. Mater. Sci.* **2006**, *51*, 881–981.
3. Zhu, Y.T.; Lowe, T.C.; Langdon, T.G. Performance and applications of nanostructured materials produced by severe plastic deformation. *Scr. Mater.* **2004**, *51*, 825–830.
4. Sakai, G.; Horita, Z.; Langdon, T.G. Grain refinement and superplasticity in an aluminum alloy processed by high-pressure torsion. *Mater. Sci. Eng. A* **2005**, *393*, 344–351.

5. Nickel, D.; Dietrich, D.; Mehner, T.; Frint, P.; Spieler, D.; Lampke, T. Effect of strain localization on pitting corrosion of an AlMgSi0.5 alloy. *Metals* **2015**, *5*, 172–191.
6. Segal, V.M. Equal channel angular extrusion: from macromechanics to structure formation. *Mater. Sci. Eng. A* **1999**, *271*, 322–333.
7. Luis, C.J. On the correct selection of the channel die in ECAP processes. *Scr. Mater.* **2004**, *50*, 387–393.
8. Kim, W.J.; Sa, Y.K.; Kim, H.K.; Yoon, U.S. Plastic forming of the equal-channel angular pressing processed 6061 aluminum alloy. *Mater. Sci. Eng. A* **2008**, *487*, 360–368.
9. Humphreys, F.J.; Hatherly, M. *Recrystallization and Related Annealing Phenomena*, 2nd ed.; Elsevier: Amsterdam, The Netherland, 2004.
10. Ferrasse, S.; Segal, V.M.; Alford, F.; Kardokus, J.; Strothers, S. Scale up and application of equal-channel angular extrusion for the electronics and aerospace industries. *Mater. Sci. Eng. A* **2008**, *493*, 130–140.
11. Altan, T.; Ngaile, G.; Shen, G. *Cold And Hot Forging: Fundamentals And Applications*, 1st ed.; ASM International: Materials Park, OH, USA, 2005.
12. Poortman, S.; Duchêne, L.; Habraken, A.M.; Verlinden, B. Modelling compression tests on aluminium produced by equal channel angular extrusion. *Acta Mater.* **2009**, *57*, 1821–1830.
13. Agena, A.S.M. A study of flow characteristics of nanostructured Al-6082 alloy produced by ECAP under upsetting test. *J. Mater. Process. Technol.* **2009**, *209*, 856–863.
14. Luis, C.J.; Puertas, I.; Salcedo, D.; León, J.; Pérez, I. Comparison between FEM and Experimental Results in the Upsetting of Nano-Structured Materials. *Mater. Sci. Forum* **2012**, *713*, 31–36.
15. Lee, J.H.; Kang, S.H.; Yang, D.Y. Novel forging technology of a magnesium alloy impeller with twisted blades of micro-thickness. *CIRP Ann. Manuf. Technol.* **2008**, *57*, 261–264.
16. Yanagida, A.; Joko, K.; Azushima, A. Formability of steels subjected to cold ECAE process. *J. Mater. Process. Technol.* **2008**, *201*, 390–394.
17. Choi, J.S.; Nawaz, S.; Hwang, S.K.; Lee, H.C.; Im, Y.T. Forgeability of ultra-fine grained aluminum alloy for bolt forming. *Int. J. Mech. Sci.* **2010**, *52*, 1269–1276.
18. Luis, C.J.; Salcedo, D.; León, J.; Puertas, I.; Fuertes, J.P.; Luri, R. Manufacturing of nanostructured rings from previously ECAE-processed AA5083 alloy by isothermal forging. *J. Nanomater.* **2013**, *2013*, 1–14.
19. Puertas, I.; Luis Pérez, C.J.; Salcedo, D.; León, J.; Fuertes, J.P.; Luri, R. Design and mechanical property analysis of AA1050 turbine blades manufactured by equal channel angular extrusion and isothermal forging. *Mater. Des.* **2013**, *52*, 774–784.
20. Luis Pérez, C.J.; Salcedo, D.; Puertas, I. Design and mechanical property analysis of ultrafine grained gears from AA5083 previously processed by equal channel angular pressing and isothermal forging. *Mater. Des.* **2014**, *63*, 126–135.
21. Vazquez, V.; Altan, T. Die design for flashless forging of complex parts. *J. Mater. Process. Tech.* **2000**, *98*, 81–89.
22. Grass, H.; Kremaszky, C.; Werner, E. 3-D FEM-simulation of hot forming processes for the production of a connecting rod. *Comput. Mater. Sci.* **2006**, *36*, 480–489.
23. Lee, M.K.; Lee, H.; Lee, T.S.; Jang, H. Buckling sensitivity of a connecting rod to the shank sectional area reduction. *Mater. Des.* **2010**, *31*, 2796–2803.

24. Shenoy, P.S.; Fatemi, A. *Connecting Rod Optimization for Weight and Cost Reduction*; SAE Technical Paper 2005-01-0987; SAE International: Warrendale, PA, USA, 2005; doi:10.4271/2005-01-0987.
25. Lewis, R. Friction in a hydraulic motor piston/cam roller contact lined with PTFE impregnated cloth. *Wear* **2009**, *266*, 888–892.
26. Khare, S.; Singh, O.P.; Dora, K.B.; Sasun, C. Spalling investigation of connecting rod. *Eng. Fail. Anal.* **2012**, *19*, 77–86.
27. Fuertes, J.P.; León, J.; Luis, C.J.; Salcedo, D.; Puertas, I.; Luri, R. Design, optimization and mechanical property analysis of a submicrometric aluminium alloy connecting rod. *J. Nanomater.* major revision required.
28. Fuertes, J.P.; Murillo, O.; León, J.; Luis, C.; Salcedo, D.; Puertas, I.; Luri, R. Mechanical properties analysis of an Al-Mg alloy connecting rod with submicrometric structure. *MESIC* **2015**, accepted.

© 2015 by the authors; licensee MDPI, Basel, Switzerland. This article is an open access article distributed under the terms and conditions of the Creative Commons Attribution license (<http://creativecommons.org/licenses/by/4.0/>).